Theor Chim Acta (1986) 70: 303-322

Theoretica Chimica Acta

Valency and molecular structure

M. S. Gopinathan, Prabha Siddarth and C. Ravimohan

Department of Chemistry, Indian Institute of Technology, Madras 600 036, India

(Received March 29 1985, revised April 17/Accepted June 23, 1986)

Valency is defined for each molecular orbital. The molecular orbital valency values are shown to be a good measure of the bonding nature of the molecular orbital. Comparisons are made with photoelectron spectral studies and Mulliken overlap population analysis.

The variation of molecular valency and molecular orbital valency with bond angle is studied. It is found that for all the molecules presently considered, energy is linearly related to valency and that the molecular valency reaches a maximum at the equilibrium bond angle. It is also shown that the molecular orbital valency can serve as a quantitatively reliable ordinate for Mulliken-Walsh diagrams.

Key words: Molecular orbital valency – Bonding nature – Mulliken–Walsh diagrams

1. Introduction

A quantum chemical definition of atomic valency in terms of the density matrix elements of the molecules has been proposed earlier [1–3]. The bond index introduced by Wiberg [4] is the basis of the valency definition. Recently a generalisation of this definition for configuration interaction calculations [5] has been given. Atomic valency finally appears as the expectation value of diatomic portions of the density operator.

In this paper, we introduce a definition of *molecular orbital valency.* Molecular orbital (MO) valency is obtained by decomposing the total valency of the molecule into its MO components. We show that the MO valency thus defined is a measure of the bonding nature of the MO. For this purpose, *ab initio* (STO-3G) results are presented for MO valencies in various diatomic and polyatomic systems and compared with predictions of the bonding nature based on photoelectron spectra (PES) and Mulliken overlap population analysis.

Further, the dependence of both molecular and molecular orbital valencies on bond angle is studied. It is found that the energy is fairly linearly related to valency in all the molecules. It is shown that the molecular valency is a maximum at the equilibrium bond angle and that the MO valency serves as a quantitative ordinate of Mulliken–Walsh diagrams [6, 7].

2. Molecular orbital valency

Valency V_A of an atom A in a molecule is defined as (see Eq. 2.14 of [3]),

$$V_A = \sum_a^A \sum_{B \neq A} \sum_b^B P_{ab}^2. \tag{2.1}$$

Here P_{ab} is the spinless density matrix element between atomic orbital a on atom A and atomic orbital b on atom B. The atomic orbitals are taken to be orthonormal. Presently we use STO-3G wavefunctions, after a Löwdin orthogonalisation [8] of the basis functions, to calculate valency.

Substituting for P_{ab} as

$$P_{ab} = \sum_i n_i C_{ia} C_{ib}$$

where C_{ia} is the coefficient of the atomic orbital a in the ith MO, Eq. (2.1) becomes,

$$V_A = \sum_i \left(\sum_a^A \sum_{B \neq A} \sum_b^B \sum_j n_i n_j C_{ia} C_{ib} C_{ja} C_{jb} \right). \tag{2.2}$$

Now the molecular valency may be defined as half the sum of atomic valencies

$$V_M = \tfrac{1}{2} \sum_A V_A. \tag{2.3}$$

The factor $\frac{1}{2}$ removes the double counting of valency between the atoms. Using Eq. (2.2), we have for the molecular valency,

$$\begin{aligned} V_M &= \sum_i \tfrac{1}{2} \sum_A \sum_a^A \sum_{B \neq A} \sum_b^B \sum_j n_i n_j C_{ia} C_{ib} C_{ja} C_{jb}. \\ &= \sum_i V_i \end{aligned} \tag{2.4}$$

Equation (2.4) expresses the molecular valency as a sum over occupied molecular orbitals. Hence, we can define V_i, the valency of the ith MO as

$$V_i = \tfrac{1}{2} \sum_A \sum_a^A \sum_{B \neq A} \sum_b^B \sum_j n_i n_j C_{ia} C_{ib} C_{ja} C_{jb}. \tag{2.5}$$

We now examine the properties of the molecular orbital valency as defined by Eq. (2.5).

Table 1. Molecular orbital valencies for homonuclear diatomics

Orbital	H_2	Li_2	N_2	F_2
$1\sigma_g$	1.000	0.006	0.004	0.002
$1\sigma_u$	—	0.004	0.001	0.002
$2\sigma_g$	—	0.998	0.777	0.308
$2\sigma_u$	—	—	0.027	0.004
$1\pi_u$	—	—	0.971	0.009
$3\sigma_g$	—	—	0.184	0.772
$1\pi_g$	—	—	—	0.007

3. Valency and bonding nature of molecular orbitals

Since valency is a measure of the extent of electron sharing between various atomic centres, we may expect the MO valency to have the following trends:

i) Zero or low values for core, anti-bonding and lone pair molecular orbitals. Note that since MO valencies are generally positive, no distinction can be made between non-bonding and anti-bonding orbitals.

ii) High values for strongly bonding molecular orbitals.

This expectation is indeed borne out by the calculated MO valencies. Presently, we have computed MO valencies for several diatomic and polyatomic molecules at their STO-3G optimised geometries. These are presesnted in Tables 1–3. The notable features of the results for all the molecules are:

1) The low value of MO valency obtained for all $1a_1$ and 1σ core orbitals. For instance, the MO valencies are 0.006, 0.004 and 0.002 for the $1\sigma_g$ orbital in Li_2, N_2 and F_2 respectively (Table 1). This is in accordance with the fact that core MO's do not take part in bonding in the sense that electrons in these are not shared among the various atoms.

The same is true of the anti-bonding MO's. For example, $2\sigma_u$ in N_2 and F_2 have small valency values (Table 1).

Table 2. Molecular orbital valencies for heteronuclear diatomics

	LiH	HF	LiF	CO	BF
1σ	0.005	0.000	0.000	0.001	0.000
2σ	1.027	0.275	0.002	0.001	0.000
3σ		0.681	0.210	0.695	0.450
4σ		—	0.279	0.140	0.313
1π		0.000	0.580	0.812	0.377
5σ				0.112	0.046

Table 3. Molecular orbital valencies for polyatomic molecules

CH_4		NH_3		H_2O			
$1a_1$	0.002	$1a_1$	0.001	$1a_1$	0.000		
$2a_1$	1.038	$2a_1$	0.887	$2a_1$	0.614		
$1t_2$	0.989	$1e$	0.999	$1b_2$	0.997		
		$3a_1$	0.086	$3a_1$	0.360		
				$1b_1$	0.000		
LiOH		Li_2O		HCN		LiCN	
1σ	0.001	$1\sigma_g$	0.001	1σ	0.002	1σ	0.003
2σ	0.007	$2\sigma_g$	0.004	2σ	0.004	2σ	0.004
3σ	0.782	$1\sigma_u$	0.001	3σ	0.866	3σ	0.002
4σ	0.831	$3\sigma_g$	0.435	4σ	0.922	4σ	0.863
1π	0.527	$1\pi_u$	0.191	5σ	0.201	5σ	0.461
		$2\sigma_u$	0.214	1π	0.999	6σ	0.601
		$2\pi_u$	0.105			1π	1.046
HCHO		C_2H_2		N_2O			
$1a_1$	0.001	1σ	0.007	1σ	0.000		
$2a_1$	0.002	2σ	0.002	2σ	0.003		
$3a_1$	0.682	3σ	0.999	3σ	0.002		
$4a_1$	0.790	4σ	0.989	4σ	0.762		
$1b_2$	0.741	5σ	0.992	5σ	0.735		
$5a_1$	0.480	1π	1.000	6σ	0.239		
$1b_1$	0.993			1π	0.716		
$2b_2$	0.371			7σ	0.225		
				2π	0.523		

The lone pair MO's also have vanishing or low valency. Thus $1b_1$ in H_2O has a valency value of zero and $3a_1$ lone pair in NH_3 has a low value of 0.086 (Table 3).

2) The bonding molecular orbitals have high MO valencies close to unity. For instance $1\sigma_g$ in H_2, $2\sigma_g$ in Li_2, $1\pi_u$ in N_2 (Table 1) and $1b_2$ in H_2O (Table 3) all have valency values approaching unity. We discuss below in more detail the MO valency values in relation to the bonding nature of molecular orbitals.

3.1. MO valencies in homonuclear diatomics

In the series of homonuclear diatomic molecules (Table 1), the value of 1.00 for $1\sigma_g$ in H_2 requires little comment. The valency of the $2\sigma_g$ in Li_2 is 0.998 indicating it to be a strongly bonding orbital. This result is supported by spectroscopic evidence in the form of ΔR_e (i.e. $R^+ - R^0$), the change in the equilibrium bond length upon ionisation, which is positive for bonding orbitals and negative for antibonding orbitals [9]. For $2\sigma_g$ of Li_2, ΔR_e value is [10] $+0.76$ Å, while theoretical calculations yield [11] a ΔR_e value of $+1.14$ Å, indicating the strongly bonding character of $2\sigma_g$. The orbital force criterion of Tal and Katriel [12] also indicates it to be bonding.

The core orbitals $1\sigma_g$ and $1\sigma_u$ have very small MO valencies as expected. In N_2, the bonding is due to the $2\sigma_g$ and $1\pi_u$ orbitals, which have valencies of 0.777 and 0.971 respectively. $3\sigma_g$ has a low valency of 0.184 indicating it to be only weakly bonding. The antibonding $2\sigma_u$ orbital has nearly zero valency. These conclusions are well supported by spectroscopic evidence. For instance, values of ΔR_e for $3\sigma_g$, $1\pi_u$ and $2\sigma_u$ in N_2 are [12] +0.04, 0.15 and −0.04 respectively. Photoelectron spectrum of N_2 shows that the band corresponding to the transition from $1\pi_u$ has extensive vibrational fine structure [13] indicating it to be a strongly bonding MO.

It may be pointed out here that the Mulliken overlap population analysis of the MO's in Li_2 and N_2 [14] lead to conclusions regarding the bonding nature of molecular orbitals in agreement with the present results based on MO valency.

In F_2, valency values indicate the $3\sigma_g$ to be the main bonding orbital (MO valency 0.772) while $2\sigma_g$ is also fairly bonding with a valency of 0.308. All other MO's have nearly zero valencies indicating them to be core, lone pairs or antibonding orbitals. Clearly this is in agreement with the conventional picture [15], where the single bond in F_2 is a σ-bond formed by the $2p_z$ orbitals on each F atom. This corresponds to the $3\sigma_g$ orbital in F_2. $1\pi_u$ and $1\pi_g$ are the lone-pairs corresponding to $2p_x$ and $2p_y$ in the free atoms and hence have almost zero valency. The $2\sigma_g$ orbital has a MO valency of 0.308 due to some s-p_z mixing. However, these results are at variance with the reported Mulliken population analysis [14] which suggests $1\pi_u$ to be the main bonding MO with somewhat less bonding for $2\sigma_g$ (MO overlap population being +0.438 and 0.356, respectively). The population analysis thus attributes a dominant π-character to the "single bond" in F_2. The Mulliken population analysis however suffers from drawbacks such as (a) strong dependence on the quality of wavefunction and (b) basis set dependence. Hybridization or the use of a basis set other than a minimal basis can introduce serious errors [14].

Presently, we have done MO overlap population analysis for a number of molecules (Table 4) using STO-3G wavefunctions. The values for $2\sigma_g$ and $1\pi_u$ in F_2 are 0.277 and 0.039, respectively. Thus the present population analysis indicates a σ bond in F_2, in agreement with the MO valency results.

The PES of F_2 [13] shows three bands which have been assigned, in increasing order of binding energy, as $1\pi_g$, $1\pi_u$ and $3\sigma_g$. $1\pi_g$ is found to be antibonding in agreement with our MO valency results. The second band is found to be strongly bonding in the PES spectrum judging from its broad nature [12]. The theoretical ordering of energy levels obtained in our STO-3G calculation, as well as those of Wahl [16] are, in increasing magnitude of eigenvalues, $1\pi_g$, $3\sigma_g$ and $1\pi_u$. Thus the second peak could theoretically correspond to $3\sigma_g$ and would be strongly bonding as per the MO valency of 0.772 (Table 1). Thus the observed strong bonding nature for the second band is reproduced by MO valency analysis; the reported assignment of the second band as $1\pi_u$ [13] therefore requires investigation. It must be emphasized that all these arguments implicitly assume the validity of the Koopmans' theorem.

Table 4. Comparison of photoelectron spectral (PES) data, Mulliken overlap populations (N_i) and MO valencies (V_i) for molecules[a]

	PES		N_i	V_i		PES		N_i	V_i
N_2[b]	$1\sigma_g$		n (0.001)	n (0.004)	C_2H_4[b]	$1a_g$		n (0.000)	n (0.004)
	$1\sigma_u$		n (0.003)	n (0.001)		$1b_{1u}$		n (−0.014)	n (0.001)
	$2\sigma_g$		s (0.852)	s (0.777)		$2a_g$	s	s (0.991)	s (0.997)
	$2\sigma_u$	n	n (−0.006)	n (0.027)		$2b_{1u}$	s	s (0.768)	s (0.983)
	$1\pi_u$	s	s (0.538)	s (0.971)		$1b_{2u}$	s	s (0.845)	s (1.001)
	$3\sigma_g$	w	n (−0.009)	w (0.184)		$3a_g$	s	s (0.602)	s (0.987)
F_2[a]	$1\sigma_g$		n (0.000)	n (0.002)		$1b_{3g}$	s	s (0.522)	s (1.004)
	$1\sigma_u$		n (0.000)	n (0.002)		$1b_{3u}$	s	s (0.885)	s (1.000)
	$2\sigma_g$		b (0.277)	b (0.308)	C_2H_2[b]	1σ		n (0.004)	n (0.007)
	$2\sigma_u$		a (−0.198)	n (0.004)		2σ		n (−0.016)	n (0.002)
	$1\pi_u$	b	n (0.039)	n (0.009)		3σ		s (0.915)	s (0.999)
	$3\sigma_g$		w (0.185)	s (0.772)		4σ	s	s (0.811)	s (0.989)
	$1\pi_g$	a	a (−0.111)	n (0.007)		5σ	s	s (0.715)	s (0.992)
CO[d]	1σ		n (−0.001)	n (0.001)		1π	s	s (0.563)	s (1.000)
	2σ		n (0.000)	n (0.001)	HCHO[b]	$1a_1$		n (−0.003)	n (0.001)
	3σ		s (0.620)	s (0.695)		$2a_1$		n (−0.005)	n (0.002)
	4σ	w	w (0.132)	w (0.140)		$3a_1$		s (0.626)	s (0.682)
	1π	s	s (0.552)	s (0.812)		$4a_1$		s (0.565)	s (0.790)
	5σ	n	a (−0.124)	n (0.112)		$1b_2$	s	s (0.681)	s (0.741)
H_2O[b]	$1a_1$		n (−0.003)	n (0.000)		$5a_1$		n (0.092)	b (0.480)
	$2a_1$		s (0.551)	s (0.614)		$1b_1$	s	b (0.349)	s (0.993)
	$1b_2$	b	s (0.578)	s (0.997)		$2b_2$	n	n (−0.049)	b (0.371)
	$3a_1$	s	n (−0.006)	b (0.360)	CO_2[b]	$1\sigma_g$		n (0.005)	n (0.001)
	$1b_1$	n	n (0.000)	n (0.000)		$1\sigma_u$		n (−0.003)	n (0.001)
NH_3[b]	$1a_1$		n (−0.001)	n (0.001)		$2\sigma_g$		n (−0.002)	n (0.002)
	$2a_1$		s (0.789)	s (0.887)		$3\sigma_g$		s (0.668)	s (0.649)
	$1e$	s	s (0.564)	s (0.999)		$2\sigma_u$		s (0.667)	s (0.656)
	$3a_1$	w	n (−0.006)	n (0.086)		$4\sigma_g$	w	b (0.272)	b (0.317)
CH_4[c]	$1a_1$		n (−0.004)	n (0.002)		$3\sigma_u$	w	w (0.189)	b (0.375)
	$1t_2$	s	s (0.619)	s (1.038)		$1\pi_u$	s	s (0.595)	s (0.709)
	$2a_1$	s	s (0.984)	s (0.989)		$1\pi_g$	n	n (−0.010)	b (0.439)

[a] The molecular orbital is designated as non-bonding (n), weakly bonding (w), bonding (b), strongly bonding (s) according to the following scheme:
n if $-0.05 < X_i \leq 0.10$
w if $0.10 < X_i \leq 0.25$
b if $0.25 < X_i \leq 0.5$
s if $0.5 < X_i$
where X_i = overlap population N_i or MO valency V_i. If $N_i \leq -0.05$, the MO is called antibonding (a). Both N_i and V_i have been presently calculated using STO-3G wavefunctions.
[b] PES data from [22]
[c] PES data from [13]
[d] PES data from [23]

3.2. MO *valencies in heteronuclear diatomics*

MO valency results for LiH, HF, LiF, BF and CO are presented in Table 2. Again the core 1σ orbitals have, as expected, valency close to zero. LiF shows considerable π bonding with 0.580 valency for 1π. All valence orbitals in LiF are quite bonding, and it is interesting that more than 50% of the bonding is due to the 1π orbital.

In CO, of the total valency of 2.57, π valency is 1.62 and σ valency is 0.95. The core orbitals 1σ and 2σ corresponding to O_{1s} and C_{1s} orbitals respectively have very small valency. 3σ and 1π are evidently bonding orbitals with valencies of 0.695 and 0.812, respectively. 4σ and 5σ are low valent with values of 0.140 and 0.112 respectively. Molecular orbitals coefficients and population according to Hartree-Fock quality wavefunctions [17, 18] confirm the present inference that 3σ and 1π are strongly bonding. These studies also show 4σ to be antibonding and 5σ to be essentially a pure carbon lone-pair orbital, in agreement with the present low valency values for these orbitals. Photoelectron spectrum of CO [13] shows a narrow peak corresponding to the ionization for 5σ orbital while the 1π band shows extensive vibrational structure. The vibrational frequency corresponding to the 5σ peak is about $2160\ \mathrm{cm}^{-1}$ which is nearly unchanged from the ground state frequency of $2170\ \mathrm{cm}^{-1}$ while the corresponding value for 1π band is very much reduced to $1610\ \mathrm{cm}^{-1}$ on ionization. The ΔR_e value for 1π is calculated [13] to be +0.11 Å. All these results firmly support the conclusions based on molecular orbital valency values.

The isoelectronic species CO and N_2 have comparable MO valency values. For example, the $2\sigma_g$ and $1\pi_u$ of N_2 which correspond to the 3σ and 1π of CO have high valencies. This is also true of the other isoelectronic species BF (Table 2). However, in the series N_2, CO, BF, the bonding due to 3σ (or $2\sigma_g$ in N_2) and 1π progressively diminishes while 4σ becomes increasingly bonding (Fig. 1). This is to be expected since along this series, the energy gap between the atomic orbitals on the two atoms combining to form the MO increases and this would make the bonding MO's less bonding and correspondingly the anti-bonding MO's less antibonding.

In HF, the results show that 3σ is strongly bonding while 2σ is moderately bonding. The 1π orbital corresponding to the $2p$ lone-pairs on F has zero valency. These results are in accordance with the PES of HF [13], which shows a broad band corresponding to 3σ and a sharp peak for 1π.

3.3. *MO valencies in polyatomic molecules*

MO valency results for several polyatomic molecules are given in Table 3. We discuss below a few typical cases.

In H_2O, the core $1a_1$ and the lone-pair $1b_1$ have zero valency as expected. The $2a_1$ and $1b_2$ orbitals are strongly bonding while $3a_1$ is moderately bonding judging from its comparatively low valency value. Predictions based on various other methods like photoelectron spectra [19], charge densities [20] and population

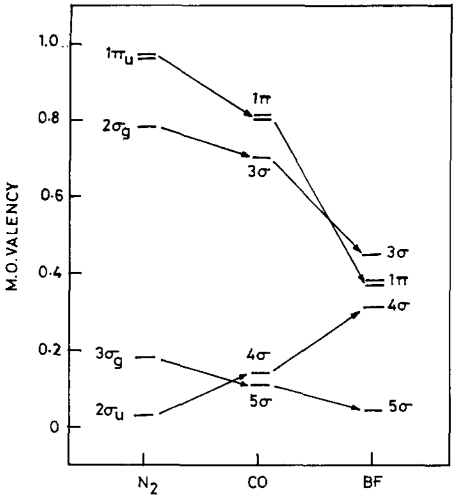

Fig. 1. Variation of MO valencies in the isoelectronic series N_2, CO, BF

studies [21] confirm the above findings. Thus the PES of H_2O [19] shows extensive vibrational structure for the $1b_2$ orbital. Bands corresponding to $2a_1$ and $3a_1$ also show similar behaviour, though to a less extent.

In the ten-electron hydride series HF, H_2O, NH_3 and CH_4, the $2a_1$ orbital (2σ in HF) is bonding and the MO valency increases in that order. Similarly the 3σ in HF which correlates with the $1b_2$, $1e$ and $1t_2$ of H_2O, NH_3 and CH_4 respectively are all strongly bonding. The bonding nature of the three topmost valence MO's in these molecules also increases from HF to CH_4 as shown in Fig. 2. This is expected in view of the increasing number of bonds being formed in this series and consequent sharing of these electrons among increasing number of atomic centres.

MO valencies for LiOH, Li_2O, HCN, LiCN, HCHO, C_2H_2 and N_2O are also given in Table 3. We shall discuss the case of HCHO as a further example of polyatomic molecule for which spectroscopic and theoretical studies are available. PES of HCHO suggests that [22] $2b_2$ is essentially non-bonding, $3a_1$ is strongly bonding between C and H and $1b_1$ is strongly C—O bonding, while $1b_2$ is bonding over the whole molecule. Valency values for $3a_1$, $1b_2$, $1b_1$ and $2b_2$ are 0.682, 0.741, 0.993 and 0.371, respectively. These values are in fair agreement with the conclusions of the analysis of the photoelectron spectrum though the valency of 0.371 for $2b_2$ seems rather high for a non-bonding orbital. Neumann and Moskowitz performed [18] *ab initio* Hartree-Fock SCF calculation on HCHO. Their molecular orbital coefficients agree well with the above MO valency predictions, with the notable exception that $4a_1$ is determined to be antibonding by their studies, whereas it has a high MO valency of 0.790.

Finally, we make a detailed comparison of the bonding power of molecular

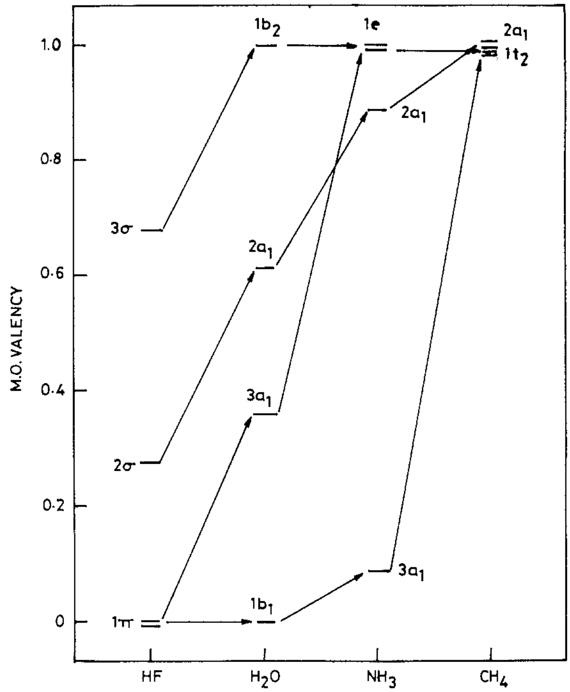

Fig. 2. Variation of MO valencies in the 10-electron hydride series HF, H_2O, NH_3 and CH_4

orbitals using the reported experimental PES measurements, overlap population analysis and MO valency values (Table 4). These three methods are found to agree quite well in most cases. However, some notable exceptions are the following.

The case of F_2 has already beeen discussed. In H_2O, the PES and the MO valency indicate $3a_1$ to be bonding, whereas the population analysis predicts it to be non-bonding. In HCHO, the $2b_2$ and $5a_1$ orbitals are seen to be bonding according to MO valency values while the other two methods indicate them to be non-bonding. Again, in CO_2, the $1\pi_g$ is predicted to be fairly well bonding by valency values whereas PES and population analysis show it to be non-bonding.

4. Variation of valency with bond angle

Since valency is a measure of the extent of electron sharing between atoms [3], it is reasonable to expect that valency will increase with increase in the amount of covalent bonding in a molecule. In this connection, it is instructive to examine the variation of valency as a function of a geometrical parameter of the molecule. In this paper, we confine our attention to bond angle variations, since we are primarily concerned with the application of MO valency to Mulliken-Walsh diagrams (Sect. 5).

First we consider the relationship between the total energy E and valency V_M of a molecule, at various bond angles. We plot $\Delta E(\theta)$, the absolute difference of the energy of the molecule at a particular bond angle θ, from the minimum energy value, i.e. $|E(\theta)-E^{\mathrm{MIN}}|$ vs $\Delta V(\theta)$ given by $|V_M(\theta)-V_M^{\mathrm{MAX}}|$, at various θ values. Such plots for several molecules are given in Fig. 3 and are seen to be linear in all cases, with the correlation coefficient values ranging from 0.985 to 0.997. Therefore, we can set

$$E(\theta)=k+lV_M(\theta) \tag{4.1}$$

where k and l are bond-angle independent constants. Admittedly, this is only a numerical result and at present we do not have any analytical proof for Eq. (4.1).

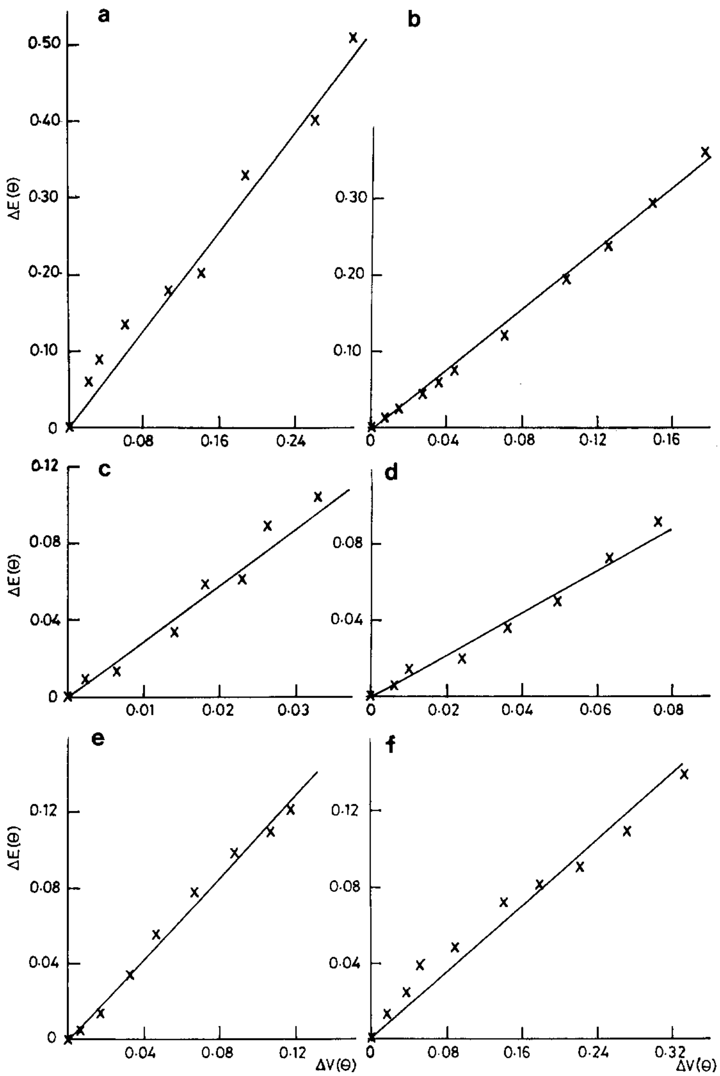

Fig. 3 a–f. Plots of $\Delta E(\theta)$ vs $\Delta V(\theta)$, as explained in the text, for **a** C_2H_2 (cis distortion) **b** CO_2 **c** NH_3 **d** C_2H_2 (trans distortion) **e** H_2O **f** HCN. The correlation coefficients are 0.995, 0.997, 0.985, 0.990, 0.993 and 0.992, respectively

From Eq. (4.1) we have

$$\frac{\partial E}{\partial \theta}=\frac{\partial V_M}{\partial \theta} \tag{4.2}$$

and further since

$$\left.\frac{\partial E}{\partial \theta}\right|_{\theta_0}=0,$$

where θ_0 is the equilibrium bond angle, it follows that

$$\left.\frac{\partial V_M}{\partial \theta}\right|_{\theta_0}=0 \tag{4.3}$$

showing that *molecular valency is an extremum at the equilibrium bond angle.* To illustrate this, valency values of several molecules at different bond angles are given in Table 5. It is clear from the table that for all the molecules presently studied, Eq. (4.3) is satisfied, at the theoretical equilibrium bond angle. Thus for linear molecules like HCN, LiCN, Li_2O and CO_2, a gradual increase in molecular valency is observed as the molecule approaches linearity from a bent structure, and V_M becomes a maximum at 180°. For H_2O, the molecular valency increases as the bond angle is increased from 75° and is the highest at 100°, which is the theoretical equilibrium bond angle. Similarly, NH_3 has its maximum molecular valency at 104.3°, its theoretical θ_0.

It would be interesting to study the variation of molecular valency with bond length to see if such an extremum principle holds there also. This might not be apparent since for example, the molecular valency of H_2, calculated using STO-3G wavefunctions constrained to be RHF, remains exactly 1.00, regardless of bond length. However, the study of valency changes with bond length probably requires wavefunctions at the CI level, since RHF wavefunctions do not, in general give the correct dissociation at large bond lengths. To confirm this, we have presently calculated molecular valency of H_2 at various bond lengths with 2 different wavefunctions which have the qualitatively correct dissociation behaviour. These are

(1) minimal basis set (STO-3G)CI wavefunction of the form [24]

$$|\Psi_{\mathrm{CI}}\rangle=\frac{1}{\sqrt{1+c^2}}[|1\sigma_g^2\rangle+c|1\sigma_u^2\rangle]$$

where $c=$ mixing coefficient of the excited state determinant. The molecular valency values of H_2 for this $|\Psi_{\mathrm{CI}}\rangle$, employing the formalism developed by Jug [5], as a function of the bond length R turn out to be: 0.950 ($1.4=R_{eq}$), 0.928 (1.6), 0.896 (1.8), 0.857 (2.0), 0.701 (2.5), 0.474 (3.0), 0.126 (4.0), 0.021 (5.0) and 0.000 (10.0) where the quantities in brackets are the R values in a.u. Thus valency decreases with increasing R, reaching the atomic limit of zero, as it should, for large R values.

Table 5. Variation of molecular valency with bond angle

Molecule	Bond angle	Molecular valency	Molecule	Bond angle	Molecular valency
H_2O	<HOH		HCN	<HCN	
	75	1.959		90	3.668
	85	1.969		100	3.775
	90	1.971		120	3.908
	95	1.972		130	3.944
	100[a]	1.973		140	3.960
	105	1.971		150	3.980
	110	1.967		160	3.988
	120	1.959		180[a]	3.995
	130	1.946	LiCN	<LiCN	
	140	1.930		100	4.013
	150	1.908		120	4.014
	160	1.885		130	4.017
	170	1.866		140	4.021
	180	1.858		150	4.023
NH_3	<HNH			160	4.026
	70	2.928		180[a]	4.027
	75	2.948	Li_2O	<LiOLi	
	80	2.960		90	0.872
	85	2.968		100	0.884
	90	2.972		120	0.909
	95	2.973		140	0.933
	100	2.973		150	0.941
	104.3[a]	2.974		160	0.948
	110	2.968		180[a]	0.952
	115	2.960	N_2O	<NNO	
	120	2.954		90	3.960
LiOH	<LiOH			120	4.102
	90	2.447		135	4.346
	100	2.467		150	4.409
	120	2.514		165	4.437
	140	2.564		180[a]	4.447
	150	2.583	CO_2	<OCO	
	160	2.599		90	4.163
	180[a]	2.615		120	4.304
FOH	<FOH			135	4.339
	80	1.971		150	4.360
	90	1.973		165	4.371
	99.3[a]	1.980		180[a]	4.374
	105	1.973	C_2H_2	<HCC	
	120	1.967	(cis distortion)	90	4.651
	150	1.926		120	4.923
	180	1.824		135	4.961
HNC	<HNC			150	4.979
	90	3.332		165	4.987
	105	3.399		180[a]	4.989
	120	3.471	C_2H_2	<HCC	
	135	3.537	(trans-		
	150	3.583	distortion)	90	4.779
	165	3.610		120	4.913
	180[a]	3.619		135	4.941

Table 5. (continued)

Molecule	Bond angle	Molecular valency	Molecule	Bond angle	Molecular valency
C_2H_2	<HCC		C_2H_4	<HCH	
(trans-				110	5.996
distortion)	150	4.966		122[a]	6.001
	165	4.984		130	5.991
	180[a]	4.989		150	5.973
	90	5.987			
	100	5.991			

[a] Theoretical equilibrium bond angle

(2) Unrestricted wavefunction of the type [24]

$$|\Psi_{\mathrm{UHF}}\rangle = |\psi_1^\alpha \psi_1^\beta \psi_2^\alpha \psi_2^\beta\rangle.$$

The unrestricted MO's are given by

$$\psi_1^{\alpha/\beta} = \cos\theta \; 1\sigma_g \pm \sin\theta \; 1\sigma_u$$

$$\psi_2^{\alpha/\beta} = \pm\sin\theta \; 1\sigma_g + \cos\theta \; 1\sigma_u.$$

Here θ incorporates a degree of freedom into the unrestricted solutions. It is sufficient to consider values of θ between 0° and 45°. The value of $\theta = 0$ corresponds to the restricted solution $\psi_1^\alpha = \psi_1^\beta = 1\sigma_g$, and at $\theta = 45°$, $\psi_1^\alpha \equiv \phi_a$, $\psi_1^\beta = \phi_b$, where ϕ_a and ϕ_b are the atomic $1s$ functions of H atoms. Thus $\theta = 45°$ corresponds to two separate H atoms. Intermediate values of θ correspond to unrestricted solutions, where ψ_1^α is mainly ϕ_a and ψ_1^β is mainly ϕ_b. Therefore as θ increases from 0° to 45°, we can consider that the bond length becomes larger and larger until it reaches the limit of isolated H atoms [24]. The values of molecular valency as a function of θ are 1.00 ($\theta = 0°$), 0.884 ($\theta = 10°$), 0.587 ($\theta = 20°$), 0.250 ($\theta = 30°$) and 0.000 ($\theta = 45°$).

Thus it is clear from the above that molecular valency does change appropriately with bond length, when proper wavefunctions are employed. We do not elaborate on this point further, since our main interest in this paper is the variation of valency with bond angle.

5. Molecular orbital valency as the ordinate of Mulliken–Walsh diagrams

Previous attempts to define the ordinate of Mulliken-Walsh (MW) diagrams [25] include Buenker and Peyerimhoff's canonical orbital eigenvalue [26], Coulson and Deb's one-electron energy quantity obtained from the Hellman-Feynman theorem [27], Stenkamp and Davidson's ICSCF eigenvalue [28] and Mehrotra and Hoffmann's tempered eigenvalue [29]. In this section, we propose to use molecular orbital valency of Eq. (2.5) as the ordinate of MW diagrams.

As shown by Eq. (4.2), the total energy θ and molecular valency V_M have the same dependence on bond angle By definition (Eq. 2.4), the sum of molecular orbital valencies yields the molecular valency. Also, the MO valency is a good measure of the bonding power of the MO in question, as shown in Sect. 3. Hence, the MO valency V_i satisfies the major requirements of the ordinate of MW diagrams. Further we note that Eq. (4.3) can be written as

$$\sum_i^{MO} \left. \frac{\partial V_i}{\partial \theta} \right|_{\theta_0} = 0$$

i.e. the sum of the slopes of the MO valency curves is zero at the equilibrium bond angle. Hence the use of MO valency as the ordinate should lead to correlation diagrams that give the exact equilibrium bond angle.

Presently, MW type diagrams with V_i as the ordinate, have been drawn for several molecules and are shown in Figs. 4, 6–12. They are in the "reduced" form, i.e. all the curves are shifted to a common origin by adding suitable constants. In doing so, we have adopted the Coulson and Deb's method of presentation [27]. It is much easier to visualise the slope of each curve in this type of diagram than in conventional plots. We observe that these diagrams, by and large, are quite similar to the original MW plots. We briefly discuss the plots for individual molecules below.

H_2O

The MO valency correlation diagram for H_2O is shown in Fig. 4. Curves for all the four valence orbitals show similar variations as in the original AH_2 Walsh diagram (Fig. 5). Thus, $2a_1$ and $1b_2$ show a negative slope indicating their preference for a linear structure. $3a_1$ curve has a steep positive slope while valency of $1b_1$ is unchanged, thus giving a net bent geometry for H_2O. We observe that equilibrium geometry can be predicted from the diagram to be 100°, where the sum of the slopes of the curves goes to zero. This may be contrasted with the

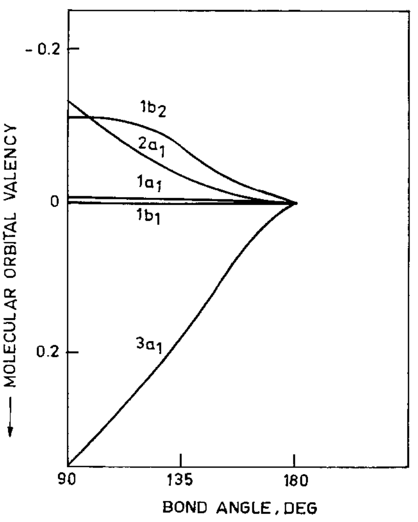

Fig. 4. MO valency correlation diagram for H_2O

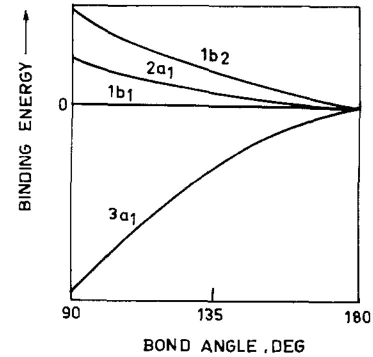

Fig. 5. Walsh diagram for AH_2 system

canonical energy plot [25] where the minimum in $\sum_i \varepsilon_i$ is not reached even at 45°. Another point of interest here is the behaviour of $2a_1$ curve. In the present case, it corresponds to the one given in the original AH_2 diagram, in contrast to the curves obtained from all the other methods [27–30]. Similarly, parallel to Walsh's reasoning, the lone pair $1b_1$ and the core $1a_1$ curves are constant with angle. Coulson and Deb [27] and Mehrotra and Hoffmann [29] obtained similar behaviour for the $1b_1$ curve but the plots of ICSCF [28] and canonical energy [30] show $1b_1$ to vary with bond angle. Also the $1a_1$ ICSCF orbital energy changes with angle. The present curve and tempered orbital energy curve for $1b_2$ orbital have small negative slopes, similar to the one in Fig. 4. However ICSCF and Couslon and Deb methods give a large negative slope for $1b_2$. Behaviour of $3a_1$ curve is quite similar in all the cases.

NH_3

The diagram for NH_3 is given in Fig. 6. It resembles closely the canonical energy plot and graphs from other methods [25, 27, 28]. In all these diagrams, $2a_1$ orbital curve has a small positive slope in contrast to that given by Walsh [7]. Again, as in the case of H_2O, we can predict the equilibrium geometry in a quantitative manner by observing that in the vicinity of bond angle value 104°, the sum of the slopes of all the curves is zero.

Li_2O

This molecule is of special interest because both Walsh [7] and canonical orbital energy plots [26] wrongly predict Li_2O to be bent while Davidson's ICSCF plot [28] correctly predicts a linear structure. The MO valency correlation diagram in the present case is given in Fig. 7 and it correctly predicts the structure to be linear. We observe that curves for all the valence orbitals have negative slopes so that all the electrons tend to keep the molecule linear.

LiOH

MO valency diagram for LiOH is given in Fig. 8. This diagram correctly predicts the geometry to be linear. $3a'$ and $4a'$ orbital curves vary slowly, with a negative

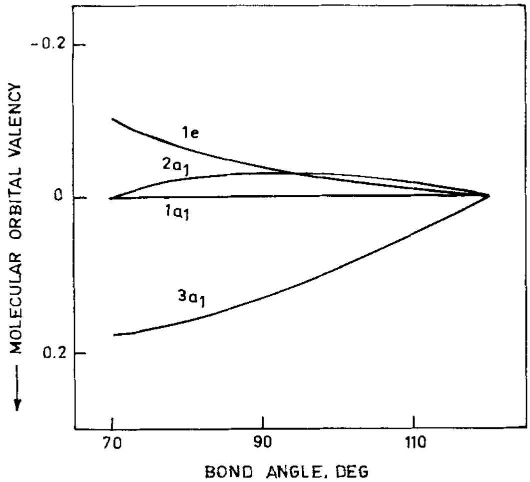

Fig. 6. MO valency correlation diagram for NH_3

slope, thus weakly indicating a linear geometry. $5a'$ has a large negative slope, thus making a large contribution towards linear geometry. $1a''$ has a positive slope, indicating a bent structure. However, its magnitude is much smaller (about half) than the slope of $5a'$ so that the molecule is linear.

HCN

The MO valency correlation diagram (Fig. 9) predicts the molecular geometry correctly to be linear. In contrast, the canonical orbital energy diagram predicts it to be bent [25]. In the present case, 3σ favours mildly bent structure, while

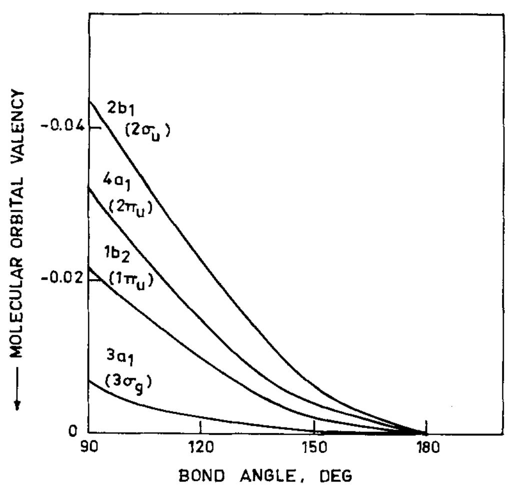

Fig. 7. MO valency correlation diagram for Li_2O

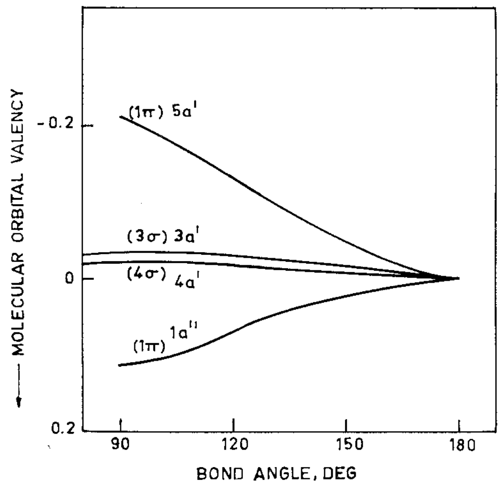

Fig. 8. MO valency correlation diagram for LiOH

4σ and 1π orbitals strongly favour linearity. 5σ favours a strongly bent shape. However, from the relative magnitudes of the slopes of the curves, it is seen that the sum of the slopes becomes zero at 180°, so that a linear structure is predicted.

HNC

Similar conclusions as in HCN can be arrived at for the case of HNC (Fig. 10). While the curves for the rest of the orbitals are slowly varying, that for $6a'$ orbital, having a large negative slope, indicates the molecule to be linear.

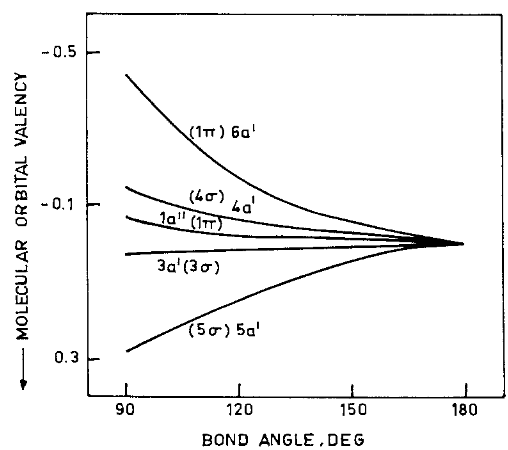

Fig. 9. MO valency correlation diagram for HCN

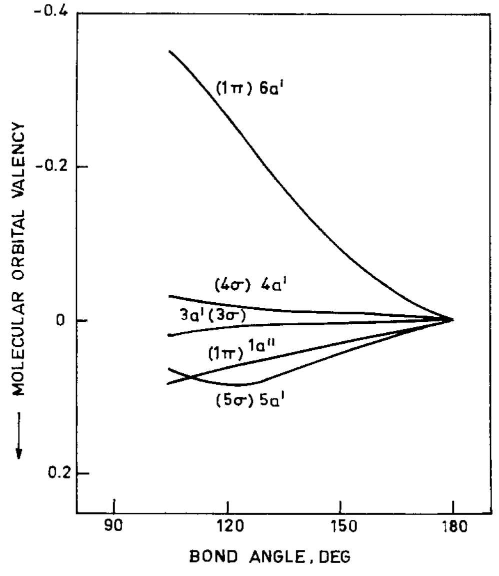

Fig. 10. MO valency correlation diagram for HNC

LiCN

Figure 11 gives the MO valency diagram for LiCN. While the rest of the orbitals vary their valency with a small slope, $6a'$ and $7a'$ have large positive and negative slopes respectively. $5a'$ weakly contributes to linearity. Overall the molecule is predicted to be linear.

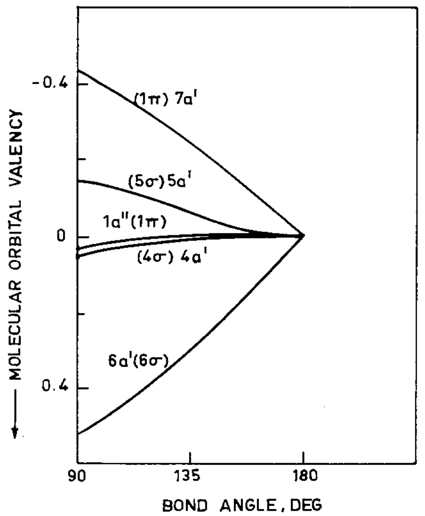

Fig. 11. MO valency correlation diagram for LiCN

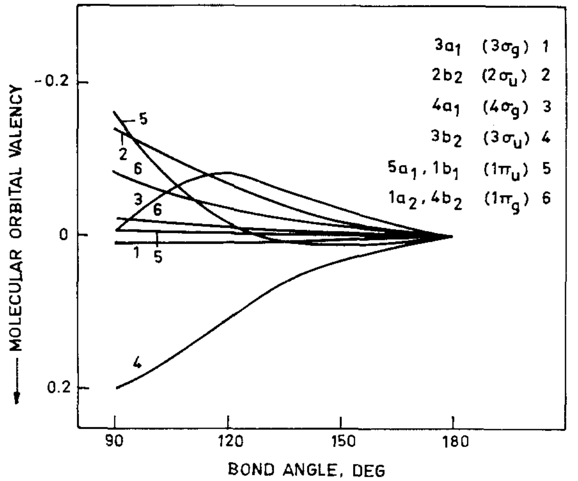

Fig. 12. MO valency correlation diagram for CO_2

CO_2

This molecule is correctly predicted to be linear by all studies. In the present model (Fig. 12), while only the $3\sigma_u$ contributes towards bent structure, all the other orbitals in general prefer linear structure. Large negative slopes are exhibited by $1\pi_u$ and $2b_2$ orbitals and these offset the large positive slope of $3b_2$. Since other orbitals show small negative slopes, the overall structure is linear. It can be observed that slopes for all the curves are zero at 180°.

6. Conclusions

Molecular orbital valency as defined presently provides a quantitative measure of the bonding nature of the molecular orbital. MO valency has a value close to unity for strongly bonding MO's and is very small for the core, lone pair and non- or anti-bonding molecular orbitals.

It is found that the total energy and valency of a molecule are linearly related and therefore the molecular valency reaches a maximum at the theoretical equilibrium bond angle. This provides a quantitative ordinate of Mulliken-Walsh diagrams in terms of the MO valency. Using MO valency as the ordinate, we have obtained correlation diagrams for a variety of molecules. These diagrams resemble the original MW diagrams quite closely and further predict the correct bond angle.

References

1. Armstrong DR, Perkins PG, Stewart JJ (1973) J Chem Soc 833:2273
2. Semenov SG (1980) In: Valency in progress. Mir Publishers, Moscow
3. Gopinathan MS, Jug K (1983) Theor Chim Acta 63: 497:511
4. Wiberg KB (1968) Tetrahedron 24: 1083

5. Jug K (1984) J Comp Chem 5; 555
6. Mulliken RS (1942) Rev Mod Phys 14: 204
7. Walsh AD (1953) J Chem Soc 2260, 2266, 2288, 2296, 2301, 2306, 2321
8. Löwdin PO (1950) J Chem Phys 18:365
9. Ferreira R (1981) Theor Chim Acta 58:131
10. Mathur BP, Rothe EW, Reck GP, Lightman AJ (1978) Chem Phys Lett 56:336
11. Clark DT, Muller J (1976) Theor Chim Acta 41:193
12. Tal Y, Katriel J (1977) Theor Chim Acta 46:173
13. Rabalais JW (1977) Principles of ultraviolet photoelectron spectroscopy. John Wiley, New York
14. Mulliken RS, Ermler WC (1977) Diatomic molecules. Academic Press, New York
15. Murrel JN, Kettle SFA, Tedder JM (1977) Valence theory. ELBS and John Wiley, London
16. Wahl AC (1964) J Chem Phys 41:2600
17. Huo W (1965) J Chem Phys 43:624
18. Neumann D, Moskowitz JW (1969) J Chem Phys 50:2216
19. Price WC, Potts AW, Streets DG (1972) In: Shirley DA (ed) Electron spectroscopy. Amsterdam, North-Holland
20. Dunning TH, Pitzer RM, Aung S (1972) J Chem Phys 57:5044
21. Neumann DB, Moskowitz JW (1968) J Chem Phys 49:2056
22. Turner DW, Baker C, Baker AP, Brundle RC (1970) Molecular photoelectron spectroscopy. Wiley-Interscience, London
23. Carlson TA (1975) Photoelectron and auger spectroscopy. Plenum Press, New York
24. Szabo A, Ostlund NS (1982) Modern quantum chemistry. MacMillan Publishing Co, New York
25. Buenker RJ, Peyerimhoff SD (1974) Chem Rev 74:127
26. Buenker RJ, Peyerimhoff SD (1966) J Chem Phys 45:3682
27. Coulson CA, Deb BM (1971) Int J Quant Chem 5:411
28. Stenkamp LZ, Davidson ER (1973) Theor Chim Acta 30:283
29. Mehrotra PK, Hoffmann R (1978) Theor Chim Acta 48:301
30. Peyerimhoff SD, Buenker RJ, Allen LC (1966) J Chem Phys 45:734